2020 IEEE/RSJ International Conference on Intelligent Robots and Systems (IROS)
October 25-29, 2020, Las Vegas, NV, USA (Virtual)

A Momentum-Based Foot Placement Strategy for Stable Postural Control of Robotic Spring-Mass Running with Point Feet

Gorkem Secer and Ali Levent Cinar

Abstract— **A long-standing argument in model-based control of locomotion is about the level of complexity that a model should have to define a behavior such as running. Even though a goldilocks model based on biomechanical evidence is often sought, it is unclear what level of complexity qualifies to be such a model. This dilemma deepens further for bipedal robotic running with point feet, since these robots are underactuated. When center-of-mass (COM) trajectories defined by the spring-loaded inverted pendulum (SLIP) model are fully tracked, angular coordinates of the robot's trunk become uncontrolled. Existing work in the literature approach this problem either by trading off COM trajectory tracking against upright trunk posture during stance or by adopting more detailed models that include effects of trunk angular dynamics. In this paper, we present a new approach based on modifying foot placement targets of the SLIP model. Theoretical analysis and numerical results show that the proposed approach can be alternative to existing strategies.**

I. INTRODUCTION

Simplified models of locomotion are widely used in robotics since they are intuitively simple and supported by biomechanical evidence. In this context, spring-loaded inverted pendulum (SLIP) model was proposed as a simple model of running [1] for natural runners that differ in number of legs, leg morphology, and posture [2]. Capturing the underlying dynamics of running [3], SLIP also serves as a target model for robotic running and hopping [4], [5], [6] since it admits extremely robust and stable running in the presence of ground height disturbances [7].

Despite these theoretical advantages of the SLIP model, it is difficult to transfer the resulting running behavior to humanoids having many degrees of freedom (DOF) including a floating-base that acts like an inverted pendulum. Angular DOF of the floating-base become uncontrolled on robots with point feet since external moments cannot be created unlike in robots with planar feet (e.g. [4]) due to the point contact whereas external forces are completely reserved for tracking trajectories defined by the SLIP. Notwithstanding the accurate realization of SLIP trajectories on the robot, uncontrolled trunk dynamics are often unstable, thus leading to failure. In the literature, there are two approaches to solve this problem: i) Optimization-based planning of center of mass (COM) trajectories which stabilizes trunk dynamics naturally instead of relying on simple models like SLIP [8], [9]. This approach actually provides a model-free solution, which requires running computationally expensive optimization algorithms at each step. Unfortunately, this is not feasibly scalable to robots with large number of DOF. As an example, interested reader can refer to CPU time results of a hybrid zero dynamics (HZD) approach for which optimization of a single gait was reported ranging from 2 to 40 seconds depending on the robot's complexity in [10]. ii) Using more detailed simple models with trunk instead of a point-mass body [11], [12], [13]. Although this is a model-based approach, it suffers from the curse of dimensionality and the lack of mechanical and intuitive interpretation of model's behavior due to the increased complexity.

In this paper, we propose an alternative approach to stabilize trunk in SLIP-like running of bipedal robots without the shortcomings of existing approaches. In this regard, our main contributions are as follows:
i) We discover that step-to-step trunk dynamics in bipedal robotic running can be formulated as a linear time-varying discrete dynamical system which admits modification of SLIP foot placement targets as a control input.
ii) We show that modifying these targets according to a linear control law provides a novel controller with provable stability guarantees.
iii) Simulations of a bipedal robot are provided to show that the proposed approach outperforms an existing model-based strategy in both transient and steady-state running.

II. THE SPRING-MASS MODEL OF RUNNING

SLIP model is basically a point-mass riding on a compliant leg, as shown in Fig. 1. Originally, the leg was modeled as a pure spring [1], which results in energetically conservative gaits. However, robotic running requires full control of the mechanical energy since a robot should be able to compensate energy losses in mechanics and to accelerate/decelerate when needed. Regarding this, different extensions to SLIP model has been proposed. In this paper, we consider the extended model in [14] since it was specifically proposed for energetically efficient control of locomotion on robotic platforms. Interested reader can see [15], [16] for other extensions of the SLIP model.

A. Model

As opposed to the original SLIP model, the extended model has a compliant leg consisting of a spring with stiffness k and rest length l_0, a damper d and a constant forcing f. Assuming that origin of the coordinate system coincides with the foot location, which is in contact with the ground during stance, dynamics take the form

$$\ddot{r}_{\text{SLIP}} = r_{\text{SLIP}}(m\|r_{\text{SLIP}}\|)^{-1}F + \begin{bmatrix}0, & -g\end{bmatrix}^T$$

Gorkem Secer is with the Laboratory of Computational Sensing and Robotics, Johns Hopkins University, Baltimore, MD, USA. Ali Levent Cinar is with the Department of Mechanical Engineering, METU, Ankara, Turkey. {gsecer@gmail.com}/{alevent.cinar@gmail.com}

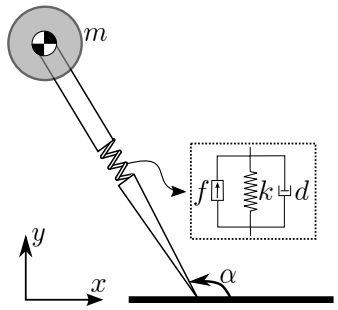

Fig. 1: Planar SLIP model with damper and constant forcing.

with $r_{\text{SLIP}} \in \mathbb{R}^2$ denoting the position of the mass m, 2-norm distance operator $\|.\|$, gravity g, and leg force

$$F = -k\left(\|r_{\text{SLIP}}\| - l_0\right) - d\left(\frac{\mathrm{d}}{\mathrm{d}t}\|r_{\text{SLIP}}\|\right) - f\,. \tag{1}$$

On the other hand, flight dynamics take the form

$$\ddot{r}_{\text{SLIP}} = \begin{bmatrix} 0, & -g \end{bmatrix}^T\,.$$

As usual, the transition between these phases are marked with touchdown and liftoff events. In particular, the stance phase starts at touchdown event marked with

$$\begin{bmatrix} 0, & 1 \end{bmatrix}\left(r_{\text{SLIP}} - \rho_{\text{td}}\right) = 0 \tag{2}$$

with

$$\rho_{\text{td}} := l_0 \begin{bmatrix} \cos(\alpha_{\text{td}}), & \sin(\alpha_{\text{td}}) \end{bmatrix}^T \tag{3}$$

denoting the foot-to-COM vector at touchdown and α_{td} denoting the touchdown leg angle. On the other hand, the liftoff event occurs when

$$F = 0\,. \tag{4}$$

B. Step-to-Step Control

The control of SLIP running is often formulated as a step-to-step regulation of apex states, which are defined as the system states at the vertically highest point (i.e., $\dot{y} = 0$) in flight. Since horizontal position is usually not a control objective in SLIP running, it can be discarded from the apex states, thus yielding their final form $Z := \begin{bmatrix} y, & \dot{x} \end{bmatrix}^T$. This definition actually provides a useful abstraction of the SLIP model by discretizing its hybrid dynamics with an apex-to-apex return map $Z_{i+1} = R(Z_i)$ from the i^{th} apex to the next. In order to control this discrete system, we consider the shifted damping strategy [14], which modifies the leg damping d and touchdown angle α_{td} once-per-step according to a deadbeat policy

$$(d, \alpha_{\text{td}}) = \arg\min \|Z_d - R(Z_i)\| \tag{5}$$

with Z_d denoting a desired apex state. While seeking a solution to these tunable parameters with this problem, we fix the leg spring to a predefined value and use the relation $f = d\left(\mathrm{d}\|r_{\text{SLIP}}\|/\mathrm{d}t\right)|_{t=t_{\text{td}}}$ proposed in [14] for the constant forcing. As a result, all parameters of the SLIP model are completely defined, hence allowing use to generate desired COM trajectories $r_{\text{SLIP}}(t)$ and foot placement targets ρ_{td} to transfer controlled running behavior to a robot.

III. BIPEDAL ROBOT MODELING AND CONTROL

As mentioned in Sec. I, control of bipedal robots with point feet is susceptible to postural instabilities due to underactuation, which is cited as the primary reason of inaccuracies in robotic running based on the SLIP model [17], [18]. To capture these effects, in this section, we consider a general bipedal robot with a trunk and point feet as a model of a target physical platform to transfer the SLIP-like running behavior described in Sec. II. To be consistent with the SLIP model, we assume that the robot is planar. Therefore, its floating-base trunk has two translational and one rotational DOF. Furthermore, similar to other instantiations of such robots [19], [5], we assume that each leg has two fully actuated DOF.

A. Model

The floating base formulation is a general framework to model a system of rigid bodies that are not fixed to the world. In this framework, for a bipedal robot whose configuration can be represented by generalized coordinates $q = \begin{bmatrix} q_b^T, & q_l^T \end{bmatrix}^T \in \mathbb{R}^7$ consisting of floating-base coordinates $q_b \in \mathrm{SE}(2)$ and joint coordinates $q_l \in \mathbb{R}^4$, dynamics take the standard form

$$M(q)\ddot{q} + C(q,\dot{q})\dot{q} + G(q) = S^T\tau + J_f^T(q)\lambda \tag{6}$$

where $M(q)$ denotes the mass matrix, $C(q,\dot{q})$ the Coriolis matrix, $G(q)$ the vector of gravitational forces, $S = \begin{bmatrix} 0_{4\times 3}, & I_{4\times 4} \end{bmatrix}$ the selection matrix mapping joint torques τ to generalized coordinates q, and the Jacobian J_f of contact constraints mapping constraint forces λ to joint space spanned by q.

The robots of interest to us have two limbs with point feet. During stance phase of a stride, one of these limbs is in contact with the ground, while the other one swings forward to prepare for the next stride. In the sequel, we will refer to them as the stance leg and as the swing leg, respectively. Because of the contact with the ground during stance, contact forces are active (i.e., $\lambda \neq 0$) with the constraint Jacobian J_f defined as the Jacobian of the stance leg's foot location $r_f(q) \in \mathbb{R}^2$ with $J_f = \partial r_f(q)/\partial q$. Furthermore, it is known that contact forces are completely determined by the joint torques during stance because of the constraint that the foot is stationary with

$$\begin{aligned} \dot{r}_f &= J_f(q)\dot{q} = 0 \\ \ddot{r}_f &= \dot{J}_f(q)\dot{q} + J_f(q)\ddot{q} = 0\,. \end{aligned} \tag{7}$$

To formulate the relation between contact forces λ and joint torques τ, we substitute the joint acceleration $\ddot{q}$ solved from (6) into (7) and obtain

$$\lambda = \left(J_f M^{-1} J_f^T\right)^{-1}\left(J_f M^{-1}(C\dot{q} + G - S^T\tau) - \dot{J}_f\dot{q}\right). \tag{8}$$

On the other hand, during flight, both legs are swinging. Hence, contact forces are not active, becoming

$$\lambda = 0\,. \tag{9}$$

Even though Equations (8) and (9) show that contact forces are indeed specified by the mode of contact and joint

torques, these forces become uncontrolled instantaneously at contact transitions. In particular, when a swing leg hits the ground, an impact happens leading to a change in states. To compute the effect of this impact on dynamics, we assume that collisions are perfectly plastic resulting in impulsive contact forces applied at the stance foot y_f. In this context, following the methodology in [20], the impact map can be written as an affine function

$$\begin{bmatrix} q^+ \\ \dot{q}^+ \end{bmatrix} = \begin{bmatrix} I_{n\times n} & 0_{n\times n} \\ 0_{n\times n} & P(q^-) \end{bmatrix} \begin{bmatrix} q^- \\ \dot{q}^- \end{bmatrix} \tag{10}$$

where $P(q)$ is the mapping between velocities prior to and posterior to the touchdown, denoted respectively with superscripts $^-$ and $^+$. In contrast to the touchdown, as the ground contact is lost, no impact occurs at the stance leg's liftoff which marks the transition from stance to flight with zero crossing of the contact force $\lambda = 0$.

B. Controls

The main objective of the controller is to transfer the SLIP running behavior to the robot. In this regard, robot's COM trajectories $r_{\text{COM}}(q) \in \mathbb{R}^2$ during flight match exactly to those of the SLIP model since flight dynamics already satisfy

$$\ddot{r}_{\text{COM}} = \ddot{r}_{\text{SLIP}} = \begin{bmatrix} 0, & -g \end{bmatrix}^T. \tag{11}$$

On the other hand, we use a feedback controller during stance to track COM trajectories of the SLIP model. Furthermore, we need to control foot positions in both phases to ensure continuous running. To achieve these goals, we adopt the Khatib's task-space control approach [21].

Consider, a vector of tasks $w(q) \in \mathbb{R}^4$, which is a function of generalized positions. Substituting joint space dynamics into task accelerations $\ddot{w} = J_w(q)\ddot{q} + \dot{J}_w(q)\dot{q}$, with Jacobian $J_w(q) = \partial w(q)/\partial q$, we obtain the task space dynamics as

$$\ddot{w} = J_w M^{-1}\left(S^T\tau + J_f^T\lambda - C\dot{q} - G\right) + \dot{J}_w\dot{q}\,. \tag{12}$$

Substituting (8) and (9) into this equation and reorganizing yields a common form for task-space dynamics as

$$\ddot{w} = E_1\left(S^T\tau - C\dot{q} - G\right) + E_2\dot{q} \tag{13}$$

$$\text{with } E_1 := \begin{cases} J_w M^{-1}(I - J_f^T(J_f M^{-1} J_f^T)^{-1} J_f M^{-1}) & \text{stance} \\ J_w M^{-1} & \text{flight} \end{cases}$$

$$E_2 := \begin{cases} \dot{J}_w - J_w M^{-1} J_f^T (J_f M^{-1} J_f^T)^{-1}\dot{J}_f & \text{stance} \\ \dot{J}_w & \text{flight}\,. \end{cases}$$

Thus, if a desired trajectory $w_d(t) \in \mathbb{R}^4$ is given, an asymptotically stable tracking controller can be formulated as

$$\tau = (E_1 S^T)^{-1}\left(\ddot{w}_d + K_d\dot{w}_e + K_p w_e + E_1(C\dot{q} + G) - E_2\dot{q}\right)$$

with controller gains $K_p \geq 0$ and $K_d \geq 0$, where $\dot{w}_e := \dot{w}_d - \dot{w}$ and $w_e := w_d - w$. This framework is sufficiently flexible to define different tasks in flight and stance phases.

Similar to [4] and [17], a state machine is employed to define and schedule these tasks depending on the mode of contact. To this end, the state machine categorizes the legs as primary and secondary. During stance, primary and secondary legs are chosen as stance and swing legs, respectively. At the lift off, they are switched so that the next stance leg is treated as the primary leg during flight. In this context, primary leg actuators are used to track SLIP's COM trajectories during stance and to realize SLIP's foot placement targets during flight. On the other hand, secondary leg basically mirrors the primary leg's motion in the horizontal direction while maintaining a safe ground clearance in the vertical direction as suggested by [22] to effectively prepare a swing leg to the next step without injecting much trunk disturbance. In order to realize these objectives, we explicitly define the task function as

$$w(q) = \left[(r_{\text{COM}}(q) - r_{f1}(q))^T, \quad (r_{\text{COM}}(q) - r_{\text{f2}}(q))^T\right]^T$$

with foot locations of the primary and secondary legs $r_{\text{f1}}(q) \in \mathbb{R}^2$ and $r_{\text{f2}}(q) \in \mathbb{R}^2$, respectively. Desired trajectory $w_d(t)$ corresponding to these tasks are defined as

$$w_d(t) = \begin{cases} \left[(r^\star_{\text{COM}}(t))^T, \quad (\rho^{\text{td}}_{\text{lo}}(t))^T\right]^T & \text{during stance} \\ \left[(\rho^{\text{td}}_{\text{lo}}(t))^T, \quad (\rho^{\text{lo}}_{\text{td}}(t))^T\right]^T & \text{during flight} \end{cases} \tag{14}$$

with $r^\star_{\text{COM}}(t) := r_{\text{SLIP}}$ and $\rho^{\text{j}}_{\text{i}}(t)$ denoting a smooth point-to-point trajectory that connects foot-to-COM position of the SLIP model at event i (i.e., ρ_i) to that at event j (i.e., ρ_j). Finally, note that, during implementation, we slightly modify these desired trajectories to avoid unwanted ground contact and discontinuities that may arise at phase transitions. However, we omit this for space reasons.

IV. TRUNK-BALANCING STRATEGIES FOR RUNNING UPRIGHT

Even though the control approach described in Sec. III-B accurately embeds the SLIP model into COM dynamics of the full robot model, it does not guarantee to stabilize the trunk orientation. Unfortunately, due to underactuation resulting from the point feet, trunk stabilization cannot be handled by trivially adding a postural task to $w(q)$ without compromising existing tasks. In the following subsections, we present a summary of the existing work and a novel strategy for balancing the trunk in the scope of spring-mass running. Note that the novel controller is our primary contribution and provides provable guarantees of postural stability by modifying foot placement targets of the SLIP model with a linear feedback law.

A. Existing Work

In the literature, there are only a few studies providing SLIP-like running with a stable trunk. Raibert [23] was the first who showed successful running experiments by allocating leg actuators for the regulation of energy and stabilization of the trunk, while foot placement is used to control forward speed. However, his controller was based on empirical observations, and the objective was to achieve steady-state running rather than single-step control accuracy. Another interesting approach [18] in the scope of HZD-based

control showed that it was possible to accurately embed both two DOF of the SLIP model and stabilize the trunk through using leg length and trunk orientation as the only tasks to control while ignoring the leg angle. However, as these results were specific to a particular robotic platform, it is not clear how they translate to robots with significant leg mass and different leg morphologies. A third approach called trunk SLIP model with virtual pendulum posture control (TSLIP-VPPC) is based on a model more detailed than the SLIP, which was originally proposed for upright human walking [13] and later adapted to running [24]. In particular, it additionally incorporates a trunk and a hip reflex. In [25] it was shown that TSLIP-VPPC achieves accurate control of running with a stable trunk. In the same paper, TSLIP-VPPC and HZD approaches were compared, and it was found that they perform similarly for a robot without leg mass. Furthermore, the performance of TSLIP-VPPC was found to be reasonably consistent for different leg masses. However, to the best of our knowledge, there is no work in the literature that investigates how HZD performs for significant leg masses. Therefore, we consider TSLIP-VPPC to compare against our approach presented in the next subsection.

TSLIP-VPPC illustrated in Fig. 2 has a finite-inertia body instead of a point-mass and applies not only forces along the compliant leg but also hip torques to stabilize the trunk. In particular, the hypothesis of [13] based on human data suggests that hip torques and leg forces are coordinated in such a way that the corresponding ground reaction force (GRF) crosses a single point fixed to the trunk throughout the stance, hence leading to pitching motion like a damped pendulum suspended from a pivot at that point. Even though this model does not completely capture trunk dynamics of robots, it has been shown to be a more useful template than the pure SLIP model by accounting for the trunk inertia which is a major contributor to the postural stability for robots with point feet.

With this extension, TSLIP-VPPC model can be described by three DOF corresponding to generalized coordinate vector $q = \begin{bmatrix} x, & y, & \theta \end{bmatrix}^T$ with COM position $\begin{bmatrix} x, & y \end{bmatrix}^T$ and trunk orientation θ. As shown in Fig. 2, compliant leg of the TSLIP-VPPC model is identical to that of the SLIP, consisting of a spring, a damper, and a constant forcing. Thus, both models produce the same leg force F given in (1) with $r_{\text{SLIP}} = r_{\text{hip}}$ corresponding to the hip location

$$r_{\text{hip}} = \begin{bmatrix} x - d_{\text{hip}} \sin\theta, & y - d_{\text{hip}} \cos\theta \end{bmatrix}^T .$$

On the other hand, in order to redirect the GRF toward the virtual pendulum pivot, hip torque

$$\tau = F \, \|r_{\text{hip}}\| \, \frac{d_{\text{hip}} \, \sin(\psi) + d_{\text{vpp}} \, \sin(\psi + \theta_{\text{vpp}})}{r - d_{\text{hip}} \, \cos(\psi) - d_{\text{vpp}} \, \cos(\psi + \theta_{\text{vpp}})}$$

is applied between the trunk and the leg, which can be defined by the angle $\psi = \alpha + \theta + \pi/2$.

Combining leg force and hip torque, stance dynamics of the TSLIP-VPPC can be expressed as

$$\ddot{q} = \text{diag}(1/m, 1/m, 1/I_b) \left(J_\psi \, \tau + J_{\text{hip}} \, F - \begin{bmatrix} 0, & mg, & 0 \end{bmatrix}^T \right)$$

with Jacobians $J_\psi := \partial\psi/\partial q$ and $J_{\text{hip}} := \partial r_{\text{hip}}/\partial q$, whereas flight dynamics take the usual form $\ddot{q} = \begin{bmatrix} 0, & -g, & 0 \end{bmatrix}^T$. These dynamics alternate with touchdown and liftoff events given in (2) and (4), respectively, yielding the return map $Z_{i+1} = R(Z_i)$ from the i^{th} apex state $Z_i = \begin{bmatrix} y, & \dot{x}, & \theta, & \dot{\theta} \end{bmatrix}^T$ to the next. Note that apex state has two more dimensions compared to the SLIP, thus requiring two more control inputs in addition to leg damping and touchdown angle in (5). Following [26], VP pivot angle θ_{vpp} and VP pivot distance d_{vpp} can be used for this purpose. Therefore, a step-to-step deadbeat policy can be formulated as

$$(\theta_{\text{vpp}}, d_{\text{vpp}}, d, \alpha_{\text{td}}) = \arg\min \|Z_d - R(Z_i)\| \qquad (15)$$

with a desired apex state Z_d. Assuming that the coordinate system coincides with the stance foot location and denoting resultant COM trajectories by $r_{\text{vpp}} = \begin{bmatrix} x, & y \end{bmatrix}^T$, the TSLIP-VPPC behavior can be translated to the robot by replacing the desired COM trajectory with $r^\star_{\text{COM}} = r_{\text{vpp}}$.

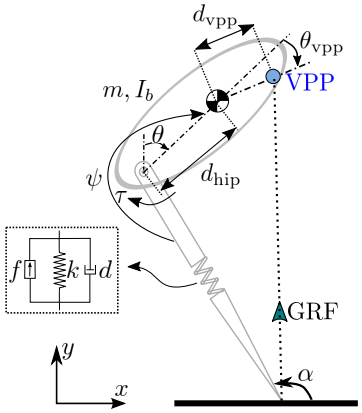

Fig. 2: TSLIP-VPPC model redirects GRF toward the VP pivot point on the body.

B. Proposed Approach : A Momentum-Based Foot Placement Strategy

Even though TSLIP-VPPC provides controlled running with stable postural dynamics, this comes at a price, as the return map's complexity increases with four dimensional state space compared to two of the SLIP model. This drastically increases both memory and computational cost of the optimization problem (15), making implementation of the controller difficult. Furthermore, in contrary to TSLIP-VPPC, the return map $R(Z_i)$ of the SLIP model admits sufficiently accurate approximate analytical solutions [15], which facilitate real-time computations. Therefore, if a solution to postural stability could be found in the scope of the SLIP model, it would be very appealing. In this regard, we propose to modify SLIP foot placement target ρ_{td} in such a way that the trunk is not unstable when SLIP trajectories are tracked on the robot.

For a given initial apex $Z_0 = \begin{bmatrix} y_0, & \dot{x}_0 \end{bmatrix}^T$, identifying horizontal and vertical components of ρ_{td} with Δx_{td} and Δy_{td},

respectively, and solving purely ballistic flight dynamics (11) yields touchdown COM states of the robot as

$$r_{\text{COM}}(q(t_{\text{td}})) = \left[\dot{x}_0\sqrt{2(y_0+\Delta y_{\text{td}})/g}, \quad -\Delta y_{\text{td}}\right]^T$$
$$\dot{r}_{\text{COM}}(q(t_{\text{td}}),\dot{q}(t_{\text{td}})) = \left[\dot{x}_0, \quad -\sqrt{2g(y_0+\Delta y_{\text{td}})}\,\right]^T .$$

As these states are determined only by the vertical component of the foot placement target, the horizontal component can be used as an additional control input. In particular, we propose to modify ρ_{td} by incorporating an offset distance Δx_u into the horizontal term in (3) as

$$\Delta x_{\text{td}} = l_0 \cos\alpha_{\text{td}} + \Delta x_u$$

to control the net moment about trunk without affecting the COM behavior. In this regard, denoting the trunk orientation states at the k^{th} apex with $\Theta_k := \left[\theta_k, \quad \dot{\theta}_k\right]^T$ and following the derivation in the Appendix, we discover that apex-to-apex trunk dynamics of a bipedal robot can be modeled as a discrete linear time-varying system

$$\Theta_{k+1} = A_k\Theta_k + B_k(\Delta x_u) + d_k \tag{16}$$

with the state transition matrix A_k, the control input-to-state matrix B_k, and the disturbance input d_k resulting from the limb movements. This formulation enables that a closed-loop controller can be designed using techniques from the feedback control theory. In this regard, as an example feedback controller in this paper, we consider a proportional-integral-derivative (PID) strategy $\Delta x_u = -K_i z_k - K_p\theta_k - K_d\dot{\theta}_k$ with integral state $z_{k+1} := z_k - \theta_k$, since disturbances can be eliminated with integral action, and since closed-loop response can be shaped as desired with PD gains. The resulting closed-loop system can be formulated as

$$\underbrace{\begin{bmatrix}\Theta_{k+1}\\ z_{k+1}\end{bmatrix}}_{\tilde{\Theta}_{k+1}} = \underbrace{\left[\begin{array}{c|c} A_k - B_kK_{pd} & -B_kK_i \\ \hline -1, \quad 0 & 0\end{array}\right]}_{A_{cl}} \underbrace{\begin{bmatrix}\Theta_k\\ z_k\end{bmatrix}}_{\tilde{\Theta}_k} + d_k$$

with $K_{pd} = \left[K_p, \quad K_d\right]$. Desired response can be obtained with formal stability guarantees by solving the eigenvalue placement problem associated with A_{cl}. Finally, we believe that the linear time-varying formulation in (16) will extend to higher DOF robots as the form of the relation (19) between angular momentum and foot placement offset will be preserved.

V. RESULTS

In this section, we present a comparison of the proposed controller with TSLIP-VPPC. In particular, controllers are compared in terms of their trunk stabilization performance alone, as our embedding approach in Sec. III-B explicitly prioritizes tracking COM trajectories over trunk stabilization, which leads to accurate COM tracking with uncontrolled trunk response, due to underactuation. Comparisons are performed for the bipedal robot illustrated in Fig. 3. The choice of this particular robot is mainly due to recent hardware platforms [27], [28] adopting the same leg morphology. While running simulations, we choose trunk mass $m_b = 60kg$,

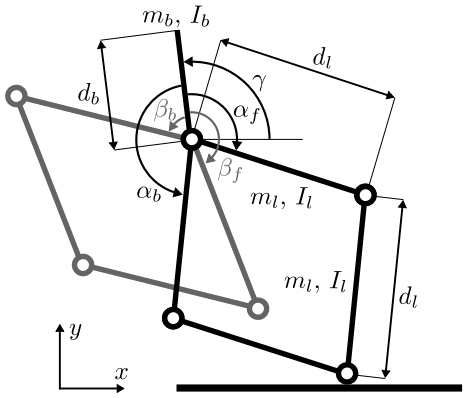

Fig. 3: Planar SLIP model with damper and constant forcing.

trunk inertia $I_b = 4.5kgm^2$, hip to trunk COM distance $d_b = 0.15m$, and link lengths $d_l = 0.5m$ of symmetric five-bar linkage legs to be compatible with the biped ATRIAS [28]. The remaining platform parameters were chosen specific to the analysis presented in the subsequent subsection.

A. Steady-State Running

By doing steady-state running experiments, we compare the postural deviation of controllers using simulations conducted across different velocities and platform parameters. In particular, we consider velocities in the range $\dot{x} \in [0,4]m/s$, while using different link masses in the range $m_l \in [0.25, 2.5]kg$ to assess the effect of leg mass on postural deviation. This is particularly important for robotic running since leg mass is a major discrepancy between hardware and simple models. However, we do not consider different apex heights but $y = 0.8m$, as we observed that height has a minimal impact on results. Note that leg links are assumed to be cylindrical in shape made out of aluminium with density $\mu = 2700kg/m^3$, defining the link inertia with $I_l = m_l(3m_l/(\pi\mu d_l) + d_l^2)/12$. Simulation results in Fig. 4 show that our approach improves the postural deviation substantially with zero steady-state error, thus guaranteeing upright running in all cases thanks to integral action, whereas TSLIP-VPPC suffers from increase in both velocity and leg mass.

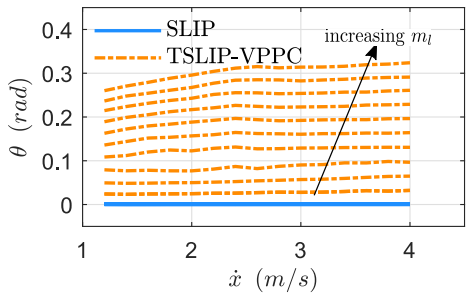

Fig. 4: Postural deviation of our approach (solid blue) and TSLIP-VPPC (dashed orange) for various speeds and masses.

B. Transient Running

As a second experiment, trunk responses of controllers are compared in an example scenario of transient running. In particular, we investigate apex-to-apex discrete behavior of the robot with nominal leg parameters (i.e., link mass $m_l = 0.5kg$ and link inertia $I_l = 0.01kgm^2$) for desired forward velocities in the range $\dot{x} \in [0,\, 4]\, m/s$, desired heights in the range $y \in [0.9, 0.72]\, m$, and desired trunk states $\theta = \dot{\theta} = 0$. In particular, the robot is commanded respectively to hop in place for 10 steps at the apex height of $0.9m$, to accelerate by $0.4m/s$ increments with $1.8cm$ decrements in apex height for 10 steps, to preserve this speed for 10 steps at the apex height of $0.72m$, to decelerate by $0.4m/s$ decrements with $1.8cm$ increments in apex height for 10 steps, and finally to come to a stop with in-place hopping at apex height of $0.9m$ for 10 steps. Results illustrated in Fig. 5 show that the proposed strategy clearly outperforms the TSLIP-VPPC by providing less postural deviation. Furthermore, results reveal interesting relations between forward speed, step-to-step acceleration and postural deviation : Being in line with the observation in Sec.V-A, postural deviation obtained with the TSLIP-VPPC seems to be correlated with the forward speed. On the other hand, there seems to be positive correlation between step-to-step acceleration and the postural deviation of the proposed approach.

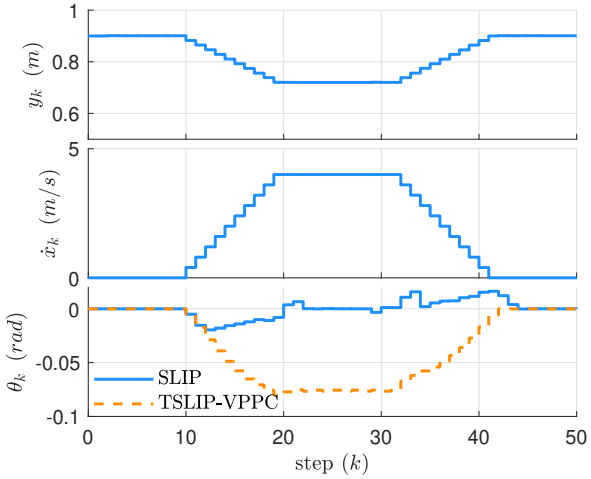

Fig. 5: Height (top), forward velocity (middle), and trunk orientation (bottom) responses at apex in each step for our approach (solid blue) and TSLIP-VPPC (dashed orange).

VI. CONCLUSIONS

In this paper, we presented a novel control approach that modifies foot placement targets defined by the simple SLIP model to stabilize trunk orientation in bipedal robotic running. To the best of our knowledge, this approach is the first strategy leading to stable trunk response without trading off tracking desired COM trajectories of SLIP running for underactuated robots with point feet. To this end, a linear controller that computes horizontal offset for foot placement target is formulated based on apex-to-apex dynamics of trunk orientation which is shown to be a discrete linear time-varying system. Finally, we show through simulations that our approach outperforms an existing strategy using a more complex locomotion model TSLIP-VPPC instead of a point-mass SLIP model to account for trunk orientation dynamics in the reference model level. Furthermore, we believe that our approach is easily scalable to 3D running as opposed other strategies favoring more complex models since they will suffer from the curse of dimensionality. For these reasons, we think that the our control approach is worth investigating on hardware platforms. In addition to verifying the theoretical/numerical results, experimental verification is also important to quantify robustness of our approach to unforeseen ground height disturbances and modeling and control errors on a real platform. As another interesting future work avenue, integration of our approach and footstep planning algorithms can be explored.

APPENDIX

In this section, we present detailed derivation of apex-to-apex trunk dynamics (16). Before doing so, however, we find it useful to present three common definitions: i) We define the centroidal angular momentum $l(t)$ (i.e., the total angular momentum about COM) as

$$l(t) := I_b\dot{\theta}(t) + \tilde{l}(t)$$

with $\tilde{l}(t)$ denoting angular momentum of limbs about the system's COM. ii) We define a simplified notation for a definite integral of centroidal angular momentum $l(t)$ as

$$L(t_0,t) := \int_{t_0}^{t} l(\tau)\mathrm{d}\tau = I_b(\theta(t_f) - \theta(t_0)) + \int_{t_0}^{t} \tilde{l}(t)\mathrm{d}t\ .$$

iii) We define a simplified notation for single and double integrals of any function $h(t)$ as

$$I(h(\tau),t_0,t) := \int_{t_0}^{t_f} h(\tau)\mathrm{d}(\tau)$$

$$D(h(\tau),t_0,t) := \int_{t_0}^{t_f} \left(\int_{t_0}^{t_f} h(\tau)\mathrm{d}\tau \right) \mathrm{d}t\ .$$

Now, suppose that initial values at the apex $\theta(0)$, $\dot{\theta}(0)$, and $\tilde{l}(0)$ are given. During flight descent phase, there are no external moments, hence, yielding

$$\begin{aligned} l(t) &= l(0) \\ L(0,t) &= l(0)t\ . \end{aligned} \tag{17}$$

Solution to trunk orientation states can be obtained from these equations as

$$\begin{aligned} \dot{\theta}(t) &= \dot{\theta}(0) + (\tilde{l}(0) - \tilde{l}(t))/I_b \\ \theta(t) &= \theta(0) + \dot{\theta}(0)t + \Delta\tilde{L}(t)/I_b \end{aligned} \tag{18}$$

with $\Delta\tilde{L}(t) = \tilde{l}(0)t - I(\tilde{l}(\tau),0,t)$.

In contrary to flight, a net moment about COM is created by GRF during stance as illustrated in Fig. 6. This can be captured by

$$\dot{l}(t) = \left(r_{\mathrm{COM}}(t) - \tilde{r}_f - [\Delta x_u,\, 0]^T\right) \otimes \left(m\ddot{r}_{\mathrm{COM}}(t) + [0,\, mg]^T\right) \tag{19}$$

with cross product $\otimes$ and unmodified foot location $\tilde{r}_f := r_{\mathrm{COM}}(t_{\mathrm{td}}) + \rho_{\mathrm{td}}$ defined by the SLIP model. Note that, for $\Delta x_u = 0$, we have

$$(r_{\mathrm{COM}}(t) - \tilde{r}_f) \otimes (m\ddot{r}_{\mathrm{COM}}(t) + [0,\, mg]^T) = 0\ ,$$

since GRF always passes through the point-mass of the SLIP model, corresponding to the robot COM. This reduces (19) to $\dot{l}(t) = \Delta x_u R_y(t)$ with $R_y(t) := -m(\ddot{y}_{\mathrm{COM}}(t) + g)$ denoting the vertical component of the force applied to the ground. Integrating this equation in stance leads to

$$\begin{aligned} l(t) &= l(t_{\mathrm{td}}) + (\Delta x_u)\, I(R_y(\tau), t_{\mathrm{td}}, t) \\ L(t_{\mathrm{td}}, t) &= l(t_{\mathrm{td}})(t - t_{\mathrm{td}}) + (\Delta x_u)\, D(R_y(\tau), t_{\mathrm{td}}, t)\ . \end{aligned} \tag{20}$$

Now, using (17) with $t = t_{\mathrm{td}}$, we obtain

$$\begin{aligned} \dot{\theta}(t) &= \dot{\theta}(0) + \left(\tilde{l}(0) - \tilde{l}(t) + (\Delta x_u)\, I(R_y(\tau), t_{\mathrm{td}}, t)\right)/I_b \\ \theta(t) &= \theta(0) + \dot{\theta}(0)t + \left(\Delta\tilde{L}(t) + (\Delta x_u)\, D(R_y(\tau), t_{\mathrm{td}}, t)\right)/I_b\ . \end{aligned}$$

Finally, we consider the flight ascent phase, during which angular momentum is conserved with

$$\begin{aligned} l(t) &= l(t_{\mathrm{lo}}) \\ L(t_{\mathrm{lo}}, t) &= l(t_{\mathrm{lo}})(t - t_{\mathrm{lo}})\ . \end{aligned} \tag{21}$$

Substituting (20) with $t = t_{\mathrm{lo}}$ into (21), trunk states are obtained as

$$\begin{aligned} \dot{\theta}(t) &= \dot{\theta}(0) + \left(\tilde{l}(0) - \tilde{l}(t)\right) + (\Delta x_u)\, I(R_y(\tau), t_{\mathrm{td}}, t_{\mathrm{lo}})\big)/I_b \\ \theta(t) &= \theta(0) + \dot{\theta}(0)t + \left(\Delta\tilde{L}(t) + (\Delta x_u)\, D(R_y(\tau), t_{\mathrm{td}}, t_{\mathrm{lo}})\right)/I_b\ . \end{aligned}$$

As we are mainly interested in apex-to-apex behavior, evaluating this equation at the stride duration $t = T_k$ and associating trunk states at $t = 0$ with the apex k and those at $t = T_k$ with the apex $k+1$ yields the time-varying linear discrete dynamical system in the state-space form

$$\underbrace{\begin{bmatrix}\theta_{k+1}\\ \dot{\theta}_{k+1}\end{bmatrix}}_{\Theta_{k+1}} = \underbrace{\begin{bmatrix}1 & T\\ 0 & 1\end{bmatrix}}_{A_k}\underbrace{\begin{bmatrix}\theta_k\\ \dot{\theta}_k\end{bmatrix}}_{\Theta_k} + \underbrace{\begin{bmatrix}D(R_y(t), t_{\mathrm{td}}, t_{\mathrm{lo}})\\ I(R_y(t), t_{\mathrm{td}}, t_{\mathrm{lo}})\end{bmatrix}}_{B_k}(\Delta x_u) + \underbrace{\begin{bmatrix}\frac{\tilde{l}(0) - \tilde{l}(T_k)}{I_b}\\ \frac{\Delta L(0, T_k)}{I_b}\end{bmatrix}}_{d_k}.$$

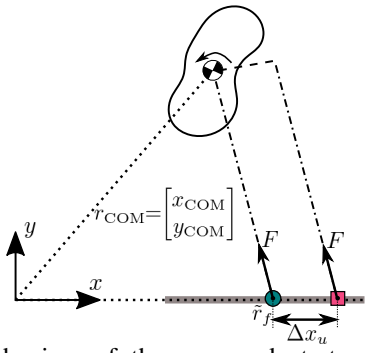

Fig. 6: Mechanism of the proposed strategy for a robot depicted as a centroidal inertia and mass with the baseline foot position $\tilde{r}_f$ and correction with horizontal shift Δx_u.

REFERENCES

[1] R. Blickhan, "The Spring-Mass Model for Running and Hopping," *Journal of Biomechanics*, vol. 22, no. 11-12, pp. 1217–1227, 1989.

[2] R. J. Full and D. E. Koditschek, "Templates and Anchors: Neuromechanical Hypotheses of Legged Locomotion," *J. of Experimental Biology*, vol. 202, pp. 3325–3332, 1999.

[3] H. Geyer, A. Seyfarth, and R. Blickhan, "Compliant Leg Behaviour Explains Basic Dynamics of Walking and Running," *Proc. of the Royal Society B*, vol. 273, no. 1603, pp. 2861–2867, 2006.

[4] P. M. Wensing and D. E. Orin, "High-Speed Humanoid Running Through Control with a 3D-SLIP Model," in *Proc. of the IEEE/RSJ Int. Conf. on Intelligent Robots and Systems*, 2013.

[5] W. C. Martin, A. Wu, and H. Geyer, "Robust Spring Mass Model Running for a Physical Bipedal Robot," in *Proc. of the IEEE Int. Conf. on Robotics and Automation*, May 2015, pp. 6307–6312.

[6] A. De and D. E. Koditschek, "Parallel Composition of Templates for Tail-Energized Planar Hopping," in *Proc. of the IEEE Int. Conf. on Robotics and Automation*, 2015.

[7] A. Wu and H. Geyer, "The 3-D Spring-Mass Model Reveals a Time-Based Deadbeat Control for Highly Robust Running and Steering in Uncertain Environments," *IEEE Transactions on Robotics*, vol. 29, no. 5, 2013.

[8] K. Sreenath, H. W. Park, I. Poulakakis, and J. W. Grizzle, "Embedding Active Force Control within the Compliant Hybrid Zero Dynamics to Achieve Stable, Fast Running on MABEL," *Int. Journal of Robotics Research*, vol. 32, no. 3, pp. 324–345, 2013.

[9] H. Dai, A. Valenzula, and R. Tedrake, "Whole-Body Motion Planning with Centroidal Dynamics and Full Kinematics," in *IEEE-RAS Int. Conf. on Humanoid Robots*, 2014.

[10] A. Hereid, C. M. Hubicki, E. A. Cousineau, and A. D. Ames, "Dynamic Humanoid Locomotion: A Scalable Formulation for HZD Gait Optimization," *IEEE Transactions on Robotics*, vol. 34, no. 2, pp. 370–387, 2018.

[11] S. H. Lee and A. Goswami, "Reaction Mass Pendulum (RMP): An Explicit Model for Centroidal Angular Momentum of Humanoid Robots," in *Proc. of the Int. Conf. on Robotics and Automation*, 2007.

[12] C. G. Atkeson and B. Stephens, "Multiple Balance Strategies From One Optimization Criterion," in *Proc. of the IEEE/RAS Int. Conf. on Humanoid Robots*, 2007.

[13] H. M. Maus, S. W. Lipfert, M. Gross, J. Rummel, and A. Seyfarth, "Upright Human Gait Did Not Provide a Major Mechanical Challenge for Our Ancestors," *Nature Communications*, vol. 1, no. 70, 2010.

[14] G. Secer and U. Saranli, "Control of Planar Spring-Mass Running Through Virtual Tuning of Radial Leg Damping," *IEEE Transactions on Robotics*, vol. 34, no. 5, pp. 1370–1383, 2018.

[15] M. M. Ankarali and U. Saranli, "Stride-to-Stride Energy Regulation for Robust Self-Stability of a Torque-Actuated Dissipative Spring-Mass Hopper," *Chaos*, vol. 20, no. 3, 2010.

[16] G. Piovan and K. Byl, "Approximation and Control of the SLIP Model Dynamics via Partial Feedback Linearization and Two-Element Leg Actuation Strategy," *IEEE Transactions on Robotics*, vol. 32, no. 2, pp. 399–412, 2016.

[17] W. C. Martin, A. Wu, and H. Geyer, "Experimental Evaluation of Deadbeat Running on the ATRIAS Biped," *IEEE Robotics and Automation Letters*, vol. 2, no. 2, pp. 1085–1092, 2017.

[18] I. Poulakakis and J. W. Grizzle, "The Spring Loaded Inverted Pendulum as the Hybrid Zero Dynamics of an Asymmetric Hopper," *IEEE Trans. on Automatic Control*, vol. 54, no. 8, pp. 1779–1793, 2009.

[19] E. R. Westervelt, J. W. Grizzle, and D. E. Koditschek, "Hybrid Zero Dynamics of Planar Bipedal Walkers," *IEEE Transactions on Automatic Control*, vol. 48, no. 1, pp. 42–56, 2003.

[20] J. W. Grizzle, G. Abba, and F. Plestan, "Asymptotically Stable Walking for Biped Robots : Analysis via Systems with Impulse Effects," *IEEE Transactions on Automatic Control*, vol. 46, no. 1, pp. 51–64, Jan. 2001.

[21] O. Khatib, "A Unified Approach for Motion and Force Control of Robot Manipulators : Operational Space Formulation," *IEEE Journal on Robotics and Automation*, vol. 3, no. 1, pp. 43–53, Feb. 1987.

[22] M. H. Raibert, *Legged Robots That Balance*. Cambridge, MA, USA: MIT Press, 1986.

[23] K. N. Murphy and M. H. Raibert, *Theory and Practice of Robots and Manipulators*. Springer, Boston, MA, 1985, ch. Trotting and Bounding in a Planar Two-Legged Model, pp. 411–420.

[24] M. Maus, J. Rummel, and A. Seyfarth, "Stable Upright Walking and Running Using a Simple Pendulum Based Control Scheme," in *Proc. of the Int. Conf. of Climbing and Walking Robots*, 2008.

[25] M. A. Sharbafi, C. Maufroy, M. N. Ahmadabadi, M. J. Yazdanpanah, and A. Seyfarth, "Robust Hopping Based on Virtual Pendulum Posture Control," *Bioinspiration & Biomimetics*, vol. 8, no. 3, 2013.

[26] M. A. Sharafi, C. Maufroy, H. M. Maus, A. Seyfarth, M. N. Ahmadabadi, and M. J. Yazdanpanah, "Controllers for Robust Hopping with Upright Trunk Based on the Virtual Pendulum Concept," in *IEEE/RSJ Int. Conf. on Intelligent Robots and Systems*, 2012.

[27] G. Kenneally, A. De, and D. E. Koditschek, "Design principles for a family of direct-drive legged robots," *IEEE Robotics and Automation Letters*, vol. 1, no. 2, pp. 900–907, 2016.

[28] C. Hubicki, J. Grimes, M. Jones, D. Renjewski, A. Sprowitz, A. Abate, and J. Hurst, "ATRIAS : Design and Validation of a Tether-Free 3D-Capable Spring-Mass Bipedal Robot," *The Int. Journal of Robotics Research*, vol. 35, no. 12, pp. 1497–1521, 2016.